

# Calculated state-of-the art results for solvation and ionization energies of thousands of organic molecules relevant to battery design

Jan Weinreich<sup>a,b,c</sup>, Konstantin Karandashev<sup>b,c,\*</sup>, Daniel Jose Arismendi Arrieta<sup>d</sup>, Kersti Hermansson<sup>d</sup>, O. Anatole von Lilienfeld<sup>e,f,g</sup>

<sup>a</sup>*Ecole Polytechnique Fédérale de Lausanne, Institut des Sciences et Ingénierie chimiques, BCH 5312 (Bât. BCH) CH-1015 Lausanne*

<sup>b</sup>*University of Vienna, Faculty of Physics, Kolingasse 14-16, AT-1090 Wien, Austria*

<sup>c</sup>*Contributed equally to this work*

<sup>d</sup>*Department of Chemistry-Ångström Laboratory, Uppsala University Box 538, 75121, Uppsala, Sweden*

<sup>e</sup>*Vector Institute for Artificial Intelligence, Toronto, ON, M5S 1M1, Canada*

<sup>f</sup>*Departments of Chemistry, Materials Science and Engineering, and Physics, University of Toronto, St. George Campus, Toronto, ON, Canada*

<sup>g</sup>*Machine Learning Group, Technische Universität Berlin and Institute for the Foundations of Learning and Data, 10587 Berlin, Germany*

---

## Abstract

We present high-quality reference data for two fundamentally important groups of molecular properties related to a compound's utility as a lithium battery electrolyte. The first one is energy changes associated with charge excitations of molecules, namely ionization potential and electron affinity. They were estimated for 7000 randomly chosen molecules with up to 9 non-hydrogen atoms C, N, O, and F (QM9 dataset) using DH-HF, DF-HF-CABS, PNO-LMP2-F12, and PNO-LCCSD(T)-F12 methods as implemented in Molpro software with aug-cc-pVTZ basis set; additionally, we provide the corresponding atomization energies at these levels of theory, as well as CPU time and disk space used during the calculations. The second one is solvation energies for 39 different solvents, which we estimate for 18361 molecules connected to battery design (Electrolyte Genome Project dataset), 309463 randomly chosen molecules with up to 17 non-hydrogen atoms C, N, O, S, and halogens (GDB17 dataset), as well as 88418 amons of ZINC database of

---

\*konstantin.karandashev@univie.ac.at

commercially available compounds and 37772 among of GDB17. For these calculations we used the COnductor-like Screening MOdel for Real Solvents (COSMO-RS) method; we additionally provide estimates of gas-phase atomization energies, as well as information about conformers considered during the COSMO-RS calculations, namely coordinates, energies, and dipole moments.

---

## 1. Introduction

Identifying candidate molecules for lithium battery electrolyte components is an important part of creating batteries suited for different modes of operation. The discovery of molecules and materials with improved functionality is expected to greatly accelerate with machine learning (ML) algorithms in coming years[35, 23, 63]. However, achieving adequate accuracy of new ML models critically depends on the availability of high-quality reference data, both for validation of the new models and of the underlying ML algorithms, and for training new models to guide exploration of chemical space. This motivated us to collect high-quality data for two fundamentally important molecular properties. The first one is energy changes associated with charge excitations of molecules, namely ionization potential and electron affinity. The second one is solvation energies which are related to how usable a compound is as an additive to lithium battery electrolytes.

Ionization potential (IP) and electron affinity (EA) are related to how readily a molecule enters reduction and oxidation reactions. Although the utility of these quantities in battery design has been put into question,[9] they are often used in preliminary screening for battery electrolyte components,[31, 11, 47, 34] where these quantities are evaluated with relatively computationally cheap calculations. Thus, our goal here is to provide accurate reference data to allow the testing of the fidelity of such calculations. When choosing our reference calculation methods, we have avoided dependence on any kind of empirical fits, disqualifying density functional theory methods and limiting our considerations to post-Hartree Fock approaches. We also aimed to balance feasible computational time for medium-sized molecules that could be considered for battery electrolytes (as too large molecules tend to create issues with solvent viscosity and ion conductivity[10]) with accuracy, drawing our attention to PNO-LMP2-F12[68, 38, 32] and PNO-LCCSD(T)-F12[54, 37, 40, 41] methods as implemented in Molpro.[69, 70, 71] The methods improve upon standard coupled-cluster method[62, 6] with single and

double excitations and a perturbative treatment of triple excitation[48, 7, 57] [CCSD(T)] and second-order Møller-Plesset perturbation theory[42, 12] (MP2) in several ways[39]. For each calculation we also present the corresponding computational time to allow using the data for developing novel multilevel machine learning schemes.[73, 20] More calculation details are given in Section 2. The resulting dataset is named “QM9-IPEA”.

Solvation energies are of similar importance for understanding interactions between the solute and the solvent, though in the context of battery research they are primarily useful for approximating trends in solubility in a given battery electrolyte,[11] with the latter quantity being a fundamentally important factor of how usable a compound is as an electrolyte additive. Our method of choice for estimating these quantities is the CONductor-like Screening MOdel for Real Solvents[29, 25, 28, 26] (COSMO-RS), which is based on quantum chemical calculations and trades a much higher cost for smaller number of additional parameters[27] and robustness. The accuracy of COSMO-RS is among the highest for describing equilibrium fluid thermodynamics: for instance, a mean unsigned error of 0.5 kcal/mol was achieved for experimental solvation energies[74] making it popular among chemical engineering applications.[18] In the context of battery material research, COSMO-RS also demonstrated reasonable mean absolute errors (as low as 0.14 V) when predicting experimental values of redox potentials.[61]

The balance of accuracy and computational cost provided by COSMO-RS allowed us to construct a dataset with a significant chemical variety of both solvated molecules and the solvents they are solvated in, while accurately reflecting physical trends over such a wide chemical space. We cover a broad spectrum of organic chemistry with our database, with a particular focus on electrolyte applications. The foundation of our database is the Electrolyte Genome Project (EGP) dataset[47], which we have expanded by randomly selecting structures from the GDB17[52] database, as well as with fragment structures of AGZ7[21] designed to cover the chemical space of ZINC and GDB17. Details are given in Section 3. Our resulting dataset contains data on 418185 molecules and is named “SolQuest”.

## 2. QM9-IPEA dataset details

### 2.1. Molecules included

The calculations were performed for a subset of the QM9[52, 49] dataset, which is often used for benchmarking in machine learning algorithm studies.

We randomly chose 7000 molecules from the dataset and performed calculations for their states with charges 0, 1, and -1 using the geometries present in the dataset. We used aug-cc-pVTZ[13, 24, 72] basis set. When running Molpro we set the following thresholds:  $10^{-8}$  a.u. for energy convergence,  $10^{-7}$  for orthonormality check,  $5 \cdot 10^{-10}$  for smallest allowed eigenvalue of the overlap matrix.

Note that calculations for 4000 of the QM9 molecules considered in this work previously appeared in Ref. 20 along with 4000 calculations for EGP.[47] We had generated the latter with exactly the same methodology, except we additionally used def2-TZVPP[64] basis set for Li, Be, and Ca atoms and aug-cc-pVTZ-PP[15, 44, 45] basis set for Zn and Br atoms.

## 2.2. *IP and EA calculations*

As mentioned in the Introduction, the local correlation treatment in PNO-LMP2-F23 and PNO-LCCSD(T)-F12 methods used here improve on the CCSD(T) method. Firstly, the scaling of the methods' cost with system size is improved by using their localized versions [LMP2[46] and LCCSD(T)[19, 53]] that only consider excitations between localized orbitals that are positioned close to each other, with such close orbitals chosen via pair natural orbital[4, 58, 56] (PNO) formalism. Secondly, since Slater determinant expansions are not well suited to reproduce cusps at points where the distance between two electrons is zero, the electron wavefunctions include a Slater-type correlation factor with the F12 approach.[59, 60] Each energy evaluation with those methods leaves as byproducts energies obtained with Hartree-Fock (HF) and HF with complementary auxiliary basis sets singles correction[3, 30] (HF-CABS). Correcting these values for the wrong cusp behavior with a density function (DF) based model[16, 36, 17] yields DH-HF and DH-HF-CABS results presented in this work. For calculating open shell species (charged molecules and individual atoms) we used restricted versions of DH-HF, DH-HF-CABS, and PNO-LMP2-F12 (DF-RHF, DFRHF-CABS, and PNO-LRMP2-F12[32]) and unrestricted versions of all Coupled Cluster methods[41] [PNO-UCCSD-F12B, PNO-UCCSD(T)-F12B, and PNO-UCCSD(T\*)-F12B].

### 3. SolQuest dataset details

#### 3.1. Molecules included

As mentioned in the introduction, we performed calculations for compounds (represented by SMILES) collected from several sources, namely the entire EGP dataset[47] of molecules connected to battery design, randomly selected compounds from the GDB17[52] dataset of molecules containing up to 17 non-hydrogen atoms (C, N, O, S, and halogens), as well as AGZ7[21]. The latter is the complete set of atom-in-molecule-based fragments[22] for GDB17 and ZINC databases restricted to no more than 7 non-hydrogen atoms; the resulting molecules include elements H, B, C, N, O, F, Si, P, S, Cl, Br, Sn, and I.

#### 3.2. Solvation free energy calculations

To keep the computational costs of creating such a dataset feasible, we turned our attention to continuum construction models,[33] in particular the COnductor-like Screening MOdel[29] (COSMO) family of solvation methods, which combined with the COSMOtherm[14] workflow only require a molecule’s SMILES for the calculation. COSMO-RS creates a solvation cavity around the solute and models solvent polarization using surface charges. These charges are derived from the solute’s electron density, which results from *ab initio* calculations in the solvent. Additionally, COSMO-RS provides insights into hydrogen bonding through charge distribution, treating the solvent as a uniform dielectric medium. The total solvation energy is evaluated based on all interactions between surface segments of solvated molecules, incorporating the likelihood of their contact, but instead of sampling individual molecule arrangements, it uses thermodynamic averages for the segments, leading to a self-consistent equation for the chemical potential.[25] By incorporating corrections for more realistic solvation simulations, COSMO-RS can model the effects of hydrogen bonds.[26] These corrections include fictitious van der Waals interactions, which are proportional to the solute’s cavity surface area, addressing the main limitations of the solvent continuum assumption.

Free energies of solvation for various common solvents (referenced in Table 7) are calculated using the Conductor-like Screening Model for Real Solvents (COSMO)[28, 26]. The calculations are processed using COSMOtherm[14], which utilizes results from prior density functional theory calculations conducted with Turbomole[55]. These calculations employ the B-P86 functional[8,

5] and the def2-TZVPD basis set[50, 8, 43, 65]. To ensure a comprehensive dataset, we use COSMOconf [2] for conformer generation. This tool features predefined procedures specifically designed to produce the most relevant conformers for COSMO-RS applications, beginning with force field-based generation, followed by clustering and diversity-based selection.

## 4. Data overview

The data is uploaded as several JavaScript Object Notation (JSON) files whose structure is discussed below.

### 4.1. QM9-IPEA

The data are kept in two JSON files, `QM9IPEA.json` and `QM9IPEA_atom_ens.json`. The former summarizes all Molpro calculations run for QM9 geometries, the latter provides atom energies necessary to recover atomization energies; the meaning of different keywords in these files is summarized in Table 1. Ionization potentials and electron affinities can be recovered as energy differences between neutral and charged (+1 for ionization potentials, -1 for electron affinities) species. `CPU_time` entries contain steps corresponding to individual method calculations, as well as steps corresponding to program operation: `INT` (calculating integrals over basis functions relevant for the calculation), `FILE` (dumping intermediate data to restart file), and `RESTART` (importing restart data). The latter two steps appeared since we reused relevant integrals calculated for neutral species in charged species’ calculations; we also used restart functionality to use HF density matrix obtained for the neutral species as the initial density matrix guess for the HF calculation for charged species. Not a number `NaN` value of a quantity means that the corresponding calculation or calculation step failed to complete. Note that the CPU times were measured while parallelizing on 12 cores and were not adjusted to single-core; they were observed on AMD Epyc 7,402 processors (24 cores, 512GB of RAM).

Distributions of main quantities of interest listed in QM9-IPEA, namely atomization energy  $E_{\text{atom}}$ , ionization energy IE, and electron affinity EA, are presented in Figure 2, with molecules featuring lowest and highest values of these quantities listed in Tables 2-4. We observe a significant difference between distributions observed for DF-HF and the other methods, whose distributions in turn look relatively similar. The tendency is underlined by

keyword	description
<b>QM9IPEA.json</b>	
COORDS	atom coordinates in Angstroms
SYMBOLS	atom element symbols
ENERGY	total energies for each charge (0, -1, 1) and method considered
CPU_TIME	CPU times (in seconds) spent at each step of each part of the calculation
DISK_USAGE	highest total disk usage in GB
ATOMIZATION_ENERGY	atomization energy at charge 0
QM9_ID	ID of the molecule in the QM9 dataset
<b>QM9IPEA_atom_ens.json</b>	
SPINS	the spin assigned to elements during calculations of atomic energies
ENERGY	energies of atoms using different methods

Table 1: Meaning of quantities found at keywords in `QM9IPEA.json` and `QM9IPEA_atom_ens.json` files. All energies are given in Hartrees with not a number (NaN) indicating the calculation failed to converge.

which molecules exhibit highest calculated properties of interest, as they agree between all methods but DF-HF.

#### 4.2. SolQuest

The dataset is presented in four JSON files listed in Table 5; they can be divided into files for full molecules of EGP and GDB17 and files for amons of GDB17 and ZINC. They are structured differently as amon entries are sorted by the number of heavy atoms in the amon (*e.g.*, all amons with 3 heavy atoms are stored in `ni3`). Because of the large number of amons with 6 or 7 heavy atoms, they are further split into `ni6_1`, `ni6_2`, etc. Apart from the calculation data the JSON files also contain Extended Connectivity Fingerprints[51] with 4 as bond radius (ECFP4) representation vectors and Simplified Molecular Input Line Entry System[66] (SMILES) strings to make them more readily usable for machine learning applications. The data is stored behind keywords listed in Table 6. For each compound, solvation energies behind the `SOLVATION` keyword additionally have one of the solvent keywords listed in Table 7. The `ENERGY` keyword denotes Boltzmann average of energy without solvent over configurations used in the solvation energy calculations. Note that the number of entries in `EGP.json`, `AMONS_GDB17.json`, and `AMONS_ZINC.json` is smaller than the number of molecules in the datasets

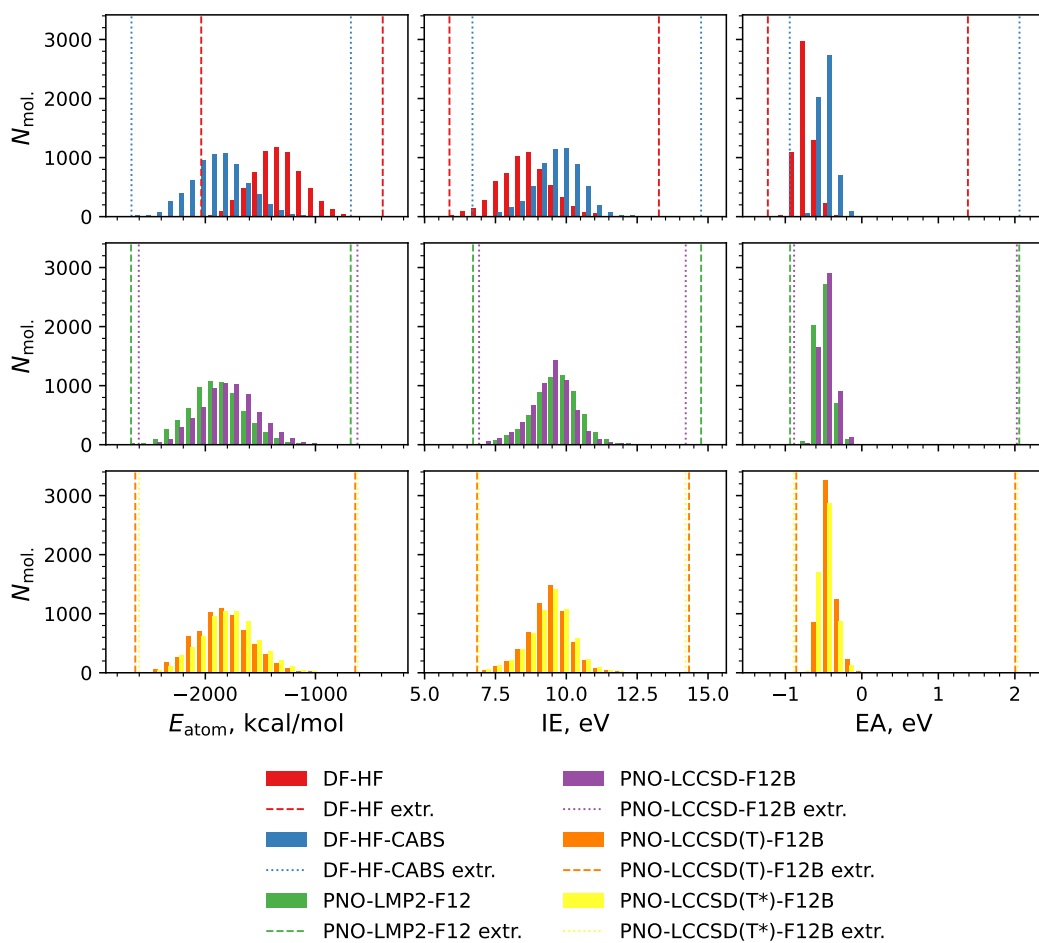


Figure 1: QM9-IPEA molecules' distributions of atomization energy  $E_{\text{atom}}$ , ionization energy IE, and electron affinity EA, as evaluated by different methods considered in this work, along with their lowest and highest values ("extr."). The latter are listed in Tables. 2-4.

method	id	SMILES	$E_{\text{atom}}$ , kcal/mol
min.			
DF-HF	121108	CCCC1CCC(C)C1	$-2.04 \cdot 10^3$
DF-HF-CABS	86195	CC1CC(C)C(C)C1C	$-2.67 \cdot 10^3$
PNO-LMP2-F12	86195	CC1CC(C)C(C)C1C	$-2.67 \cdot 10^3$
PNO-LCCSD-F12B	121108	CCCC1CCC(C)C1	$-2.60 \cdot 10^3$
PNO-LCCSD(T)-F12B	121108	CCCC1CCC(C)C1	$-2.64 \cdot 10^3$
PNO-LCCSD(T*)-F12B	121108	CCCC1CCC(C)C1	$-2.60 \cdot 10^3$
max.			
DF-HF	3839	N=C1N=NNN=N1	$-3.89 \cdot 10^2$
DF-HF-CABS	827	FC(F)(F)C#N	$-6.78 \cdot 10^2$
PNO-LMP2-F12	827	FC(F)(F)C#N	$-6.80 \cdot 10^2$
PNO-LCCSD-F12B	827	FC(F)(F)C#N	$-6.19 \cdot 10^2$
PNO-LCCSD(T)-F12B	827	FC(F)(F)C#N	$-6.39 \cdot 10^2$
PNO-LCCSD(T*)-F12B	827	FC(F)(F)C#N	$-6.17 \cdot 10^2$

Table 2: Lowest ("min.") and highest ("max.") values of atomization energy  $E_{\text{atom}}$  in QM9-IPEA for each method, along with the QM9 index ("id") of the molecule for which it was observed and the latter's SMILES.

method	id	SMILES	IE, eV
min.			
DF-HF	28102	<chem>CC1=CC2=C(N1)C=CC2</chem>	5.88
DF-HF-CABS	101807	<chem>[NH3+]CC(O)CCC([O-])=O</chem>	6.69
PNO-LMP2-F12	101807	<chem>[NH3+]CC(O)CCC([O-])=O</chem>	6.71
PNO-LCCSD-F12B	24464	<chem>N1C=CC2=CC=CC2=C1</chem>	6.92
PNO-LCCSD(T)-F12B	101807	<chem>[NH3+]CC(O)CCC([O-])=O</chem>	6.85
PNO-LCCSD(T*)-F12B	24464	<chem>N1C=CC2=CC=CC2=C1</chem>	6.91
max.			
DF-HF	99424	<chem>COC(C#N)(C#N)C#N</chem>	13.27
DF-HF-CABS	827	<chem>FC(F)(F)C#N</chem>	14.76
PNO-LMP2-F12	827	<chem>FC(F)(F)C#N</chem>	14.76
PNO-LCCSD-F12B	827	<chem>FC(F)(F)C#N</chem>	14.21
PNO-LCCSD(T)-F12B	827	<chem>FC(F)(F)C#N</chem>	14.33
PNO-LCCSD(T*)-F12B	827	<chem>FC(F)(F)C#N</chem>	14.21

Table 3: Lowest and highest values of ionization energy IE in QM9-IPEA for each method, fields labeled analogously to Table 2.

method	id	SMILES	EA, eV
min.			
DF-HF	827	<chem>FC(F)(F)C#N</chem>	-1.23
DF-HF-CABS	827	<chem>FC(F)(F)C#N</chem>	$-9.42 \cdot 10^{-1}$
PNO-LMP2-F12	827	<chem>FC(F)(F)C#N</chem>	$-9.37 \cdot 10^{-1}$
PNO-LCCSD-F12B	827	<chem>FC(F)(F)C#N</chem>	$-8.85 \cdot 10^{-1}$
PNO-LCCSD(T)-F12B	827	<chem>FC(F)(F)C#N</chem>	$-8.57 \cdot 10^{-1}$
PNO-LCCSD(T*)-F12B	827	<chem>FC(F)(F)C#N</chem>	$-8.89 \cdot 10^{-1}$
max.			
DF-HF	23832	<chem>FC1=NC(=O)ON=N1</chem>	1.39
DF-HF-CABS	130729	<chem>O=C1NN=NC(=N1)C#N</chem>	2.06
PNO-LMP2-F12	130729	<chem>O=C1NN=NC(=N1)C#N</chem>	2.06
PNO-LCCSD-F12B	130729	<chem>O=C1NN=NC(=N1)C#N</chem>	2.03
PNO-LCCSD(T)-F12B	130729	<chem>O=C1NN=NC(=N1)C#N</chem>	2.00
PNO-LCCSD(T*)-F12B	130729	<chem>O=C1NN=NC(=N1)C#N</chem>	2.03

Table 4: Lowest and highest values of electron affinity EA in QM9-IPEA for each method, fields labeled analogously to Table 2.

file name	description	num. entries	num. molecules
AMONS_GDB17.json	GDB17 amons	37860	37772
AMONS_ZINC.json	ZINC amons	88771	88418
GDB17.json	subset of GDB17	309468	309463
EGP.json	EGP molecules	18362	18361
-	total	454461	453450

Table 5: Names of files containing SolQuest data, along with number of entries and non-repeating molecules that each file contains, and the total number of entries and non-repeating molecules.

keyword	description
ECFP	ECFP4 representation vector
SMILES	SMILES string
SYMBOLS	atomic symbols
COORDS	atomic positions for each conformer in Angstrom
ATOMIZATION	atomization energy of each conformer in kcal/mol
DIPOLE	dipole moments and dipole vectors, both for each conformer, in Debye
ENERGY	average energy in Hartree
SOLVATION	solvation energies in kcal/mol for different solvents at 300 K

Table 6: Meaning of quantities found at keywords in JSON files with the COSMO-RS results.

from which they were taken because we excluded molecules for which the calculations failed. The difference between number of entries and number of molecules is due to repetitions of the same molecule inside and between the four subsets of SolQuest; the numbers of unique molecules were obtained by comparing canonical SMILES generated by RdKit[1].

We plot distributions of solvation energies  $E_{\text{solv}}$  in water, pentane, and acetonitrile (chosen as the most and the least polar solvents, and the solvent whose dielectric constant is closest to the middle between the ones of water and pentane) along with total energy  $E_{\text{tot}}$  (values behind the **ENERGY** keyword) in Figure 2, with the lowest and highest values of these quantities presented separately in Tables 8 and 9. As expected, for solvation energy values tend to become more spread out as the polarity of the solvent increases. We also see that of the among the four subsets of SolQuest’s molecules EGP

1,2-dichloroethane	ch2cl2	h2o
1,2-dimethylbenzene	chcl3	hexamethylphosphoramide
1,3-dimethylbenzene	chlorobenzene	hexane
1,4-dimethylbenzene	cyclohexane	methanol
1-butanol	diethyleneglycol	n-heptane
1-octanol	diethylether	nitromethane
2-butanol	diglyme	pentane
2-propanol	dimethylsulfoxide	propanol
aceticacid	dioxane	propanone
acetonitrile	ethanol	pyridine
benzene	ethylacetate	thf
butanone	glycerol	toluene
ccl4	glycol	triethylamine

Table 7: List of keywords corresponding to different solvents considered in this work.

molecules were the most diverse in terms of distribution of both  $E_{\text{solv}}$  and  $E_{\text{tot}}$ . Tables 8 and 9 indicate presence of outliers for which COSMO-RS calculations seemingly broke down, yielding unreasonable solvation energy values; we decided to not exclude such points from the dataset and leave it up to the end user to decide whether they are useful.

## 5. Data availability

The GitHub repository containing all scripts that were used to generate and process the data can be found at <https://github.com/chemspacelab/VienUppDa>, with the processed data uploaded to Zenodo [67] at <https://zenodo.org/records/13952172>.

## Acknowledgement

This project has received funding from the European Union’s Horizon 2020 research and innovation programme under grant agreement No 957189 (BIG-MAP) and No 957213 (BATTERY 2030+). O.A.v.L. has received funding from the European Research Council (ERC) under the European Union’s Horizon 2020 research and innovation programme (grant agreement

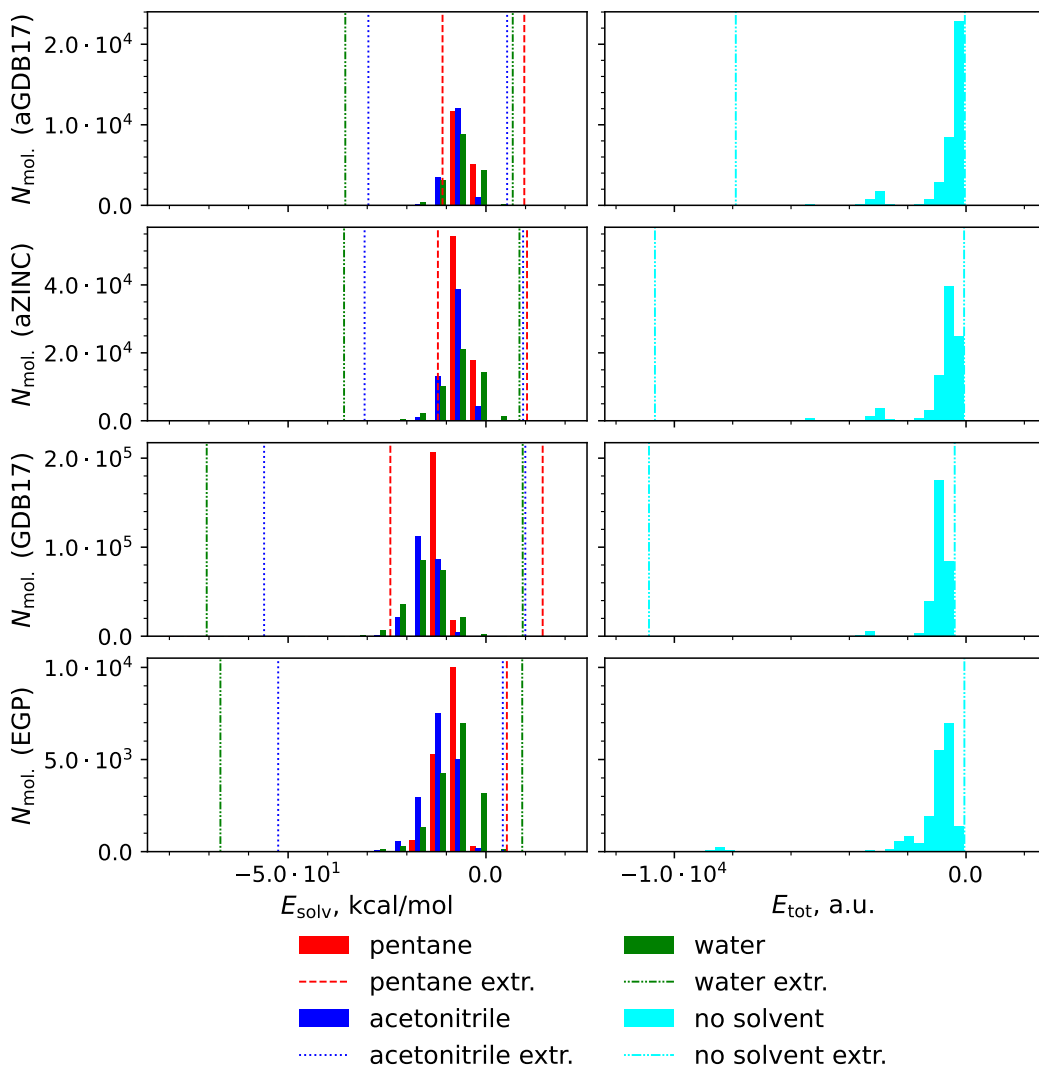


Figure 2: SolQuest molecules' distributions of solvation energies  $E_{\text{solv}}$  for pentane, acetonitrile, and water, as well as total energies without solvent  $E_{\text{tot}}$  (see explanation of ENERGY keyword in Subsec. 4.2 for definition); vertical lines denote lowest and highest ("extr.") observed values for each quantity. The latter are listed in Tables 8 and 9. The distributions are presented for the four subsets of SolQuest based on the dataset the SMILES had been taken from; for brevity "aGDB17" and "aZINC" denote "GDB17 amons" and "ZINC amons".

source dataset	solvent	SMILES	$E_{\text{solv}}$ , kcal/mol
min			
GDB17 amons	pentane	<chem>NC(=[NH2+])S(=O)(=O)[O-]</chem>	$-1.10 \cdot 10^1$
	acetonitrile	<chem>NC(=[NH2+])S(=O)(=O)[O-]</chem>	$-2.97 \cdot 10^1$
	water	<chem>NCCS(=O)(=O)O</chem>	$-3.55 \cdot 10^1$
ZINC amons	pentane	<chem>CN(C)C=[NH2+].[Cl-]</chem>	$-1.21 \cdot 10^1$
	acetonitrile	<chem>NC(=[NH2+])[C@H](N)Cl.[Cl-]</chem>	$-3.07 \cdot 10^1$
	water	<chem>NC1=[NH+]CP([O-])C1</chem>	$-3.59 \cdot 10^1$
GDB17	pentane	<chem>C[C@@]12[C@@H](C#N)C[C@@H](C/N=C\[NH-])[C@H]3C[N@@H+]1[C@@H]2[C@@H]3O</chem>	$-2.42 \cdot 10^1$
	acetonitrile	<chem>[H]/N=C(\C)[C@@H]1O[C@@H]([C-](C#N)C#C)OC[C@@H]1C[NH3+]</chem>	$-5.61 \cdot 10^1$
	water	<chem>C[C@]12[NH2+][C@H]1CNC1=N[C@@]3(CN)C#C([O-])[C@H]3[C@@H]12</chem>	$-7.06 \cdot 10^1$
EGP	pentane	<chem>[C-]#[N+]C(=O)C1=C=C=c2c3c4c(c5c(=O)c5c5sc6c7c(=O)c7c1c2c6c45)C(C(=O)[N+]#[C-])=C=C=3</chem>	$-1.66 \cdot 10^2$
	acetonitrile	<chem>[NH3+][C@@H]1CC[C@@H](C(=O)[O-])C1</chem>	$-5.25 \cdot 10^1$
	water	<chem>[NH3+][C@@H]1CC[C@@H](C(=O)[O-])C1</chem>	$-6.71 \cdot 10^1$
max			
GDB17 amons	pentane	<chem>N=C=O.NC=S</chem>	9.69
	acetonitrile	<chem>NC/C=C\C(=O)Br</chem>	5.35
	water	<chem>NC=O.S=C=NS</chem>	6.77
ZINC amons	pentane	<chem>C=C[C@H](S)ON</chem>	$1.04 \cdot 10^1$
	acetonitrile	<chem>O=CNC=O.[H]/N=N/[H]</chem>	9.39
	water	<chem>C=C(S)C[C@@H]1CS1</chem>	8.47
GDB17	pentane	<chem>CC/N=C1/NC=C2C1=NC(SC#N)=C2O.N#N</chem>	$1.43 \cdot 10^1$
	acetonitrile	<chem>CC[C@@H]1[C@]2(OC)CC=CC(=O)[C@]12N(C)C</chem>	9.94
	water	<chem>Cc1c[nH]c(=O)sc(CCN)c(/N=C/N)cn1</chem>	9.28
EGP	pentane	<chem>CN(C)[C@@]1([N+](=O)[O-])CSCCS1</chem>	5.29
	acetonitrile	<chem>O=C(O)c1cccc(O)c1O</chem>	4.26
	water	<chem>CN(C)[C@@H]1C=CSC(c2cccc2)=C1</chem>	9.17

Table 8: Lowest ("min.") and highest ("max.") values of solvation energy  $E_{\text{solv}}$  in different subsets of SolQuest for pentane, acetonitrile, and water, along with the corresponding SMILES.

source dataset	SMILES	$E_{\text{tot}}$ , a.u.
min		
GDB17 amons	<chem>Br/C=N/C(Br)=C\Br</chem>	$-7.89 \cdot 10^3$
ZINC amons	<chem>BrC(Br)[SiH2]C(Br)Br</chem>	$-1.07 \cdot 10^4$
GDB17	<chem>C[C@@H](C)N(C)C(=O)c1c(Br)nc(Br)c(Br)c1Br</chem>	$-1.09 \cdot 10^4$
EGP	<chem>BrC(Br)(Br)C1=CS/C(=C2/SC=C(C(Br)(Br)Br)S2)S1</chem>	$-1.73 \cdot 10^4$
max		
GDB17 amons	<chem>C</chem>	$-4.05 \cdot 10^1$
ZINC amons	<chem>BC</chem>	$-6.60 \cdot 10^1$
GDB17	<chem>CC1=CC(C)(C)COC1</chem>	$-3.89 \cdot 10^2$
EGP	<chem>N</chem>	$-5.66 \cdot 10^1$

Table 9: Lowest ("min.") and highest ("max.") values of total energy  $E_{\text{tot}}$  (see explanation of **ENERGY** keyword in main text for definition) in different subsets of SolQuest along with the corresponding SMILES.

No. 772834). O.A.v.L. has received support as the Ed Clark Chair of Advanced Materials and as a Canada CIFAR AI Chair. O.A.v.L. acknowledges that this research is part of the University of Toronto's Acceleration Consortium, which receives funding from the Canada First Research Excellence Fund (CFREF). Obtaining the presented computational results has been facilitated using the queueing system implemented at <http://leruli.com>. The project has been supported by the Swedish Research Council (Vetenskapsrådet), and the Swedish National Strategic e-Science program eSENCE as well as by computing resources from the Swedish National Infrastructure for Computing (SNIC/NAISS). The computational results presented have been achieved using the Vienna Scientific Cluster (VSC).

## References

- [1] , RDKit: Open-source cheminformatics. <https://www.rdkit.org>.
- [2] 3DS, . COSMOCONF: A flexible tool box for conformer generation. <https://www.3ds.com/fileadmin/PRODUCTS-SERVICES/BIOVIA/PDF/BIOVIA-cosmoconf-datasheet.pdf>.
- [3] Adler, T.B., Knizia, G., Werner, H.J., 2007. A simple and efficient CCSD(T)-F12 approximation. *J. Chem. Phys.* 127, 221106. URL: <https://doi.org/10.1063/1.2817618>, doi:10.1063/1.2817618.
- [4] Ahlrichs, R., Driessler, F., 1975. Direct determination of pair natural orbitals: A new method to solve the multi-configuration hartree-fock problem for two-electron wave functions. *Theor. Chim. Acta* 36, 275–287. URL: <https://doi.org/10.1007/BF00549691>, doi:10.1007/BF00549691.
- [5] Ahlrichs, R., Furche, F., Grimme, S., 2000. Comment on 'Assessment of exchange correlation functionals' [A. J. Cohen, N. C. Handy, *Chem. Phys. Lett.* 316 (2000) 160-166]. *Chem. Phys. Lett.* 325, 317–321. doi:10.1016/S0009-2614(00)00654-0.
- [6] Bartlett, R.J., 1989. Coupled-cluster approach to molecular structure and spectra: a step toward predictive quantum chemistry. *J. Phys. Chem.* 93, 1697–1708. URL: <https://doi.org/10.1021/j100342a008>, doi:10.1021/j100342a008.

- [7] Bartlett, R.J., Watts, J., Kucharski, S., Noga, J., 1990. Non-iterative fifth-order triple and quadruple excitation energy corrections in correlated methods. *Chem. Phys. Lett.* 165, 513–522. URL: [https://doi.org/10.1016/0009-2614\(90\)87031-L](https://doi.org/10.1016/0009-2614(90)87031-L), doi:10.1016/0009-2614(90)87031-L.
- [8] Becke, A.D., 1988. Density-functional exchange-energy approximation with correct asymptotic behavior. *Phys. Rev. A* 38, 3098–3100. URL: <https://link.aps.org/doi/10.1103/PhysRevA.38.3098>, doi:10.1103/PhysRevA.38.3098.
- [9] Borodin, O., 2019. Challenges with prediction of battery electrolyte electrochemical stability window and guiding the electrode – electrolyte stabilization. *Curr. Opin. Electrochem.* 13, 86–93. URL: <https://doi.org/10.1016/j.coelec.2018.10.015>.
- [10] Borodin, O., Olguin, M., Spear, C.E., Leiter, K.W., Knap, J., 2015. Towards high throughput screening of electrochemical stability of battery electrolytes. *Nanotechnology* 26, 354003. URL: <https://doi.org/10.1088/0957-4484/26/35/354003>.
- [11] Cheng, L., Assary, R.S., Qu, X., Jain, A., Ong, S.P., Rajput, N.N., Persson, K., Curtiss, L.A., 2015. Accelerating electrolyte discovery for energy storage with high-throughput screening. *J. Phys. Chem. Lett.* 6, 283–291. URL: <https://doi.org/10.1021/jz502319n>.
- [12] Cremer, D., 2011. Møller–Plesset perturbation theory: from small molecule methods to methods for thousands of atoms. *WIREs Comput. Mol. Sci.* 1, 509–530. URL: <https://doi.org/10.1002/wcms.58>, doi:10.1002/wcms.58.
- [13] Dunning, T.H., 1989. Gaussian basis sets for use in correlated molecular calculations. I. the atoms boron through neon and hydrogen. *J. Chem. Phys.* 90, 1007–1023. URL: <https://doi.org/10.1063/1.456153>, doi:10.1063/1.456153.
- [14] Eckert, F., Klamt, A., 2018. COSMOtherm. BIOVIA COSMOtherm, Release 2021; Dassault Systèmes. <http://www.3ds.com>.

- [15] Figgen, D., Rauhut, G., Dolg, M., Stoll, H., 2005. Energy-consistent pseudopotentials for group 11 and 12 atoms: adjustment to multi-configuration Dirac-Hartree-Fock data. *J. Chem. Phys.* 311, 227–244. URL: <https://doi.org/10.1016/j.chemphys.2004.10.005>, doi:10.1016/j.chemphys.2004.10.005.
- [16] Giner, E., Pradines, B., Ferté, A., Assaraf, R., Savin, A., Toulouse, J., 2018. Curing basis-set convergence of wave-function theory using density-functional theory: A systematically improvable approach. *J. Chem. Phys.* 149, 194301. URL: <https://doi.org/10.1063/1.5052714>, doi:10.1063/1.5052714.
- [17] Giner, E., Scemama, A., Loos, P.F., Toulouse, J., 2020. A basis-set error correction based on density-functional theory for strongly correlated molecular systems. *J. Chem. Phys.* 152, 174104. URL: <https://doi.org/10.1063/5.0002892>, doi:10.1063/5.0002892.
- [18] Grensemann, H., Gmehling, J., 2005. Performance of a conductor-like screening model for real solvents model in comparison to classical group contribution methods. *Industrial & Engineering Chemistry Research* 44, 1610–1624. doi:10.1021/ie049139z.
- [19] Hampel, C., Werner, H., 1996. Local treatment of electron correlation in coupled cluster theory. *J. Chem. Phys.* 104, 6286–6297. URL: <https://doi.org/10.1063/1.471289>, doi:10.1063/1.471289.
- [20] Heinen, S., Khan, D., von Rudorff, G.F., Karandashev, K., Arismendi Arrieta, D.J., Price, A.J.A., Nandi, S., Bhowmik, A., Hermansson, K., von Lilienfeld, O.A., 2023. Reducing training data needs with minimal multilevel machine learning (M3L). *arXiv* , 2308.11196 URL: <https://arxiv.org/abs/1706.01825>.
- [21] Huang, B., von Lilienfeld, O.A., 2020a. Dictionary of 140k GDB and ZINC derived AMONs. *arXiv*:2008.05260.
- [22] Huang, B., von Lilienfeld, O.A., 2020b. Quantum machine learning using atom-in-molecule-based fragments selected on the fly. *Nature Chemistry* 12, 945–951. URL: <https://www.nature.com/articles/s41557-020-0544-y>, doi:<https://doi.org/10.1038/s41557-020-0544-y>.

- [23] Jha, S., Yen, M., Soto, Y.S., Palmer, E., Villafuerte, J., Liang, H., 2023. Machine learning-assisted materials development and device management in batteries and supercapacitors: performance comparison and challenges. *J. Mater. Chem. A* 11, 3904–3936. URL: <http://dx.doi.org/10.1039/D2TA07148G>, doi:10.1039/D2TA07148G.
- [24] Kendall, R.A., Dunning, T.H., Harrison, R.J., 1992. Electron affinities of the first-row atoms revisited. systematic basis sets and wave functions. *J. Chem. Phys.* 96, 6796–6806. URL: <https://doi.org/10.1063/1.462569>, doi:10.1063/1.462569.
- [25] Klamt, A., 1995. Conductor-like screening model for real solvents: A new approach to the quantitative calculation of solvation phenomena. *J. Phys. Chem.* 99, 2224–2235. doi:10.1021/j100007a062.
- [26] Klamt, A., Eckert, F., 2000. Cosmo-rs: a novel and efficient method for the a priori prediction of thermophysical data of liquids. *Fluid Phase Equilibria* 172, 43–72. URL: <http://www.sciencedirect.com/science/article/pii/S0378381200003575>, doi:[https://doi.org/10.1016/S0378-3812\(00\)00357-5](https://doi.org/10.1016/S0378-3812(00)00357-5).
- [27] Klamt, A., Eckert, F., Arlt, W., 2010. COSMO-RS: An alternative to simulation for calculating thermodynamic properties of liquid mixtures. *Annual Review of Chemical and Biomolecular Engineering* 1, 101–122. doi:10.1146/annurev-chembioeng-073009-100903.
- [28] Klamt, A., Mennucci, B., Tomasi, J., Barone, V., Curutchet, C., Orozco, M., Luque, F.J., 2009. On the performance of continuum solvation methods. a comment on “universal approaches to solvation modeling”. *Acc. Chem. Research* 42, 489–492. doi:10.1021/ar800187p.
- [29] Klamt, A., Schüürmann, G., 1993. Cosmo: a new approach to dielectric screening in solvents with explicit expressions for the screening energy and its gradient. *J. Chem. Soc., Perkin Trans. 2* , 799–805 URL: <http://dx.doi.org/10.1039/P29930000799>, doi:10.1039/P29930000799.
- [30] Knizia, G., Werner, H.J., 2008. Explicitly correlated rmp2 for high-spin open-shell reference states. *J. Chem. Phys.* 128, 154103. URL: <https://doi.org/10.1063/1.2889388>, doi:10.1063/1.2889388.

- [31] Korth, M., 2014. Large-scale virtual high-throughput screening for the identification of new battery electrolyte solvents: evaluation of electronic structure theory methods. *Phys. Chem. Chem. Phys.* 16, 7919–7926. URL: <https://doi.org/10.1039/C4CP00547C>.
- [32] Krause, C., Werner, H.J., 2019. Scalable electron correlation methods. 6. local spin-restricted open-shell second-order Møller–Plesset perturbation theory using pair natural orbitals: PNO-RMP2. *Journal of Chemical Theory and Computation* 15, 987–1005. URL: <https://doi.org/10.1021/acs.jctc.8b01012>, doi:10.1021/acs.jctc.8b01012, arXiv:<https://doi.org/10.1021/acs.jctc.8b01012>.
- [33] Levine, I., 2014. *Quantum Chemistry*. Pearson advanced chemistry series, Pearson.
- [34] Lian, C., Liu, H., Li, C., Wu, J., 2019. Hunting ionic liquids with large electrochemical potential windows. *AIChE J.* 65, 804–810. URL: <https://doi.org/10.1002/aic.16467>.
- [35] Liu, Y., Guo, B., Zou, X., Li, Y., Shi, S., 2020. Machine learning assisted materials design and discovery for rechargeable batteries. *Energy Storage Mater.* 31, 434–450. URL: <https://doi.org/10.1016/j.ensm.2020.06.033>, doi:10.1016/j.ensm.2020.06.033.
- [36] Loos, P.F., Pradines, B., Scemama, A., Toulouse, J., Giner, E., 2019. A density-based basis-set correction for wave function theory. *J. Phys. Chem. Lett.* 10, 2931–2937. URL: <https://doi.org/10.1021/acs.jpcllett.9b01176>, doi:10.1021/acs.jpcllett.9b01176. PMID: 31090432.
- [37] Ma, Q., Schwilk, M., Köppl, C., Werner, H.J., 2017. Scalable electron correlation methods. 4. parallel explicitly correlated local coupled cluster with pair natural orbitals (PNO-LCCSD-F12). *Journal of Chemical Theory and Computation* 13, 4871–4896. URL: <https://doi.org/10.1021/acs.jctc.7b00799>, doi:10.1021/acs.jctc.7b00799. PMID: 28898081.
- [38] Ma, Q., Werner, H.J., 2015. Scalable electron correlation methods. 2. parallel PNO-LMP2-F12 with near linear scaling in the molecular size. *J. Chem. Theory Comput.* 11, 5291–5304. URL: <https://doi.org/10.1021/acs.jctc.5b01012>.

org/10.1021/acs.jctc.5b00843, doi:10.1021/acs.jctc.5b00843,  
arXiv:<https://doi.org/10.1021/acs.jctc.5b00843>. PMID:  
26574323.

- [39] Ma, Q., Werner, H.J., 2018a. Explicitly correlated local coupled-cluster methods using pair natural orbitals. *WIREs Comput. Mol. Sci.* 8, e1371. URL: <https://doi.org/10.1002/wcms.1371>, doi:10.1002/wcms.1371.
- [40] Ma, Q., Werner, H.J., 2018b. Scalable electron correlation methods. 5. parallel perturbative triples correction for explicitly correlated local coupled cluster with pair natural orbitals. *Journal of Chemical Theory and Computation* 14, 198–215. URL: <https://doi.org/10.1021/acs.jctc.7b01141>, doi:10.1021/acs.jctc.7b01141. PMID: 29211961.
- [41] Ma, Q., Werner, H.J., 2020. Scalable electron correlation methods. 7. local open-shell coupled-cluster methods using pair natural orbitals: PNO-RCCSD and PNO-UCCSD. *Journal of Chemical Theory and Computation* 16, 3135–3151. URL: <https://doi.org/10.1021/acs.jctc.0c00192>, doi:10.1021/acs.jctc.0c00192. PMID: 32275428.
- [42] Møller, C., Plesset, M.S., 1934. Note on an approximation treatment for many-electron systems. *Phys. Rev.* 46, 618–622. URL: <https://doi.org/10.1103/PhysRev.46.618>, doi:10.1103/PhysRev.46.618.
- [43] Perdew, J.P., 1986. Density-functional approximation for the correlation energy of the inhomogeneous electron gas. *Phys. Rev. B* 33, 8822–8824. URL: <https://link.aps.org/doi/10.1103/PhysRevB.33.8822>, doi:10.1103/PhysRevB.33.8822.
- [44] Peterson, K.A., Figgen, D., Goll, E., Stoll, H., Dolg, M., 2003. Systematically convergent basis sets with relativistic pseudopotentials. II. small-core pseudopotentials and correlation consistent basis sets for the post-d group 16-18 elements. *J. Chem. Phys.* 119, 11113–11123. URL: <https://doi.org/10.1063/1.1622924>, doi:10.1063/1.1622924.
- [45] Peterson, K.A., Puzzarini, C., 2005. Systematically convergent basis sets for transition metals. II. pseudopotential-based correlation consistent basis sets for the group 11 (Cu, Ag, Au) and 12 (Zn, Cd, Hg) elements.

- Theor. Chem. Acc. 114, 283–296. URL: <https://doi.org/10.1007/s00214-005-0681-9>, doi:10.1007/s00214-005-0681-9.
- [46] Pulay, P., Saebø, S., 1986. Orbital-invariant formulation and second-order gradient evaluation in Møller-Plesset perturbation theory. *Theor. Chim. Acta* 69, 357–368. URL: <https://doi.org/10.1007/BF00526697>, doi:10.1007/BF00526697.
- [47] Qu, X., Jain, A., Rajput, N.N., Cheng, L., Zhang, Y., Ong, S.P., Brafman, M., Maginn, E., Curtiss, L.A., Persson, K.A., 2015. The Electrolyte Genome Project: A big data approach in battery materials discovery. *Comput. Mater. Sci.* 103, 56–67. URL: <https://doi.org/10.1016/j.commatsci.2015.02.050>.
- [48] Raghavachari, K., Trucks, G.W., Pople, J.A., Head-Gordon, M., 1989. A fifth-order perturbation comparison of electron correlation theories. *Chem. Phys. Lett.* 157, 479–483. URL: [https://doi.org/10.1016/S0009-2614\(89\)87395-6](https://doi.org/10.1016/S0009-2614(89)87395-6), doi:10.1016/S0009-2614(89)87395-6.
- [49] Ramakrishnan, R., Dral, P.O., Rupp, M., von Lilienfeld, O.A., 2014. Quantum chemistry structures and properties of 134 kilo molecules. *Sci. Data* 1, 140022. URL: <https://doi.org/10.1038/sdata.2014.22>.
- [50] Reinisch, J., Diedenhofen, M., Wilcken, R., Udvarhelyi, A., Glöß, A., 2019. Benchmarking different QM levels for usage with COSMO-RS. *Journal of Chemical Information and Modeling* 59, 4806–4813. doi:10.1021/acs.jcim.9b00659.
- [51] Rogers, D., Hahn, M., 2010. Extended-connectivity fingerprints. *J. Chem. Inf. Model.* 50, 742–754. URL: <https://doi.org/10.1021/ci100050t>, doi:10.1021/ci100050t. PMID: 20426451.
- [52] Ruddigkeit, L., van Deursen, R., Blum, L.C., Reymond, J.L., 2012. Enumeration of 166 billion organic small molecules in the chemical universe database GDB-17. *J. Chem. Inf. Model.* 52, 2864–2875. URL: <https://doi.org/10.1021/ci300415d>.
- [53] Schütz, M., Werner, H.J., 2000. Local perturbative triples correction (t) with linear cost scaling. *Chem. Phys. Lett.* 318, 370–378. URL: [https://doi.org/10.1016/S0009-2614\(00\)00066-X](https://doi.org/10.1016/S0009-2614(00)00066-X), doi:S0009-2614(00)00066-X.

- [54] Schwilk, M., Ma, Q., Köppl, C., Werner, H.J., 2017. Scalable electron correlation methods. 3. efficient and accurate parallel local coupled cluster with pair natural orbitals (PNO-LCCSD). *J. Chem. Theory Comput.* 13, 3650–3675. URL: <https://doi.org/10.1021/acs.jctc.7b00554>, doi:10.1021/acs.jctc.7b00554. PMID: 28661673.
- [55] software, . TURBOMOLE V7.2 2017, a development of University of Karlsruhe and Forschungszentrum Karlsruhe GmbH, 1989-2007, TURBOMOLE GmbH, since 2007; available from <http://www.turbomole.com>.
- [56] Staemmler, V., Jaquet, R., 1981. CEPA calculations on open-shell molecules. I. Outline of the method. *Theor. Chim. Acta* 59, 129–145. URL: <https://doi.org/10.1007/BF00938691>, doi:10.1007/BF00938691.
- [57] Stanton, J.F., 1997. Why CCSD(T) works: a different perspective. *Chem. Phys. Lett.* 281, 130–134. URL: [https://doi.org/10.1016/S0009-2614\(97\)01144-5](https://doi.org/10.1016/S0009-2614(97)01144-5), doi:10.1016/S0009-2614(97)01144-5.
- [58] Taylor, P.R., 1981. A rapidly convergent CI expansion based on several reference configurations, using optimized correlating orbitals. *J. Chem. Phys.* 74, 1256–1270. URL: <https://doi.org/10.1063/1.441186>, doi:10.1063/1.441186.
- [59] Ten-no, S., 2004a. Explicitly correlated second order perturbation theory: Introduction of a rational generator and numerical quadratures. *J. Chem. Phys.* 121, 117–129. URL: <https://doi.org/10.1063/1.1757439>, doi:10.1063/1.1757439.
- [60] Ten-no, S., 2004b. Initiation of explicitly correlated Slater-type geminal theory. *Chem. Phys. Lett.* 398, 56–61. URL: [10.1016/j.cplett.2004.09.041](https://doi.org/10.1016/j.cplett.2004.09.041), doi:<https://doi.org/10.1016/j.cplett.2004.09.041>.
- [61] Tomaník, L., Rulíšek, L., Slavíček, P., 2023. Redox potentials with COSMO-RS: Systematic benchmarking with different databases. *J. Chem. Theory Comput.* 19, 1014–1022. doi:10.1021/acs.jctc.2c00919.
- [62] Čížek, J., 1966. On the correlation problem in atomic and molecular systems. calculation of wavefunction components in Ursell-type expansion

- using quantum-field theoretical methods. *J. Chem. Phys.* 45, 4256–4266. URL: <https://doi.org/10.1063/1.1727484>, doi:10.1063/1.1727484.
- [63] Wang, Z., Wang, L., Zhang, H., Xu, H., He, X., 2024. Materials descriptors of machine learning to boost development of lithium-ion batteries. *Nano Converg.* 11. URL: <https://doi.org/10.1186/s40580-024-00417-6>, doi:10.1186/s40580-024-00417-6.
- [64] Weigend, F., Ahlrichs, R., 2005a. Balanced basis sets of split valence, triple zeta valence and quadruple zeta valence quality for H to Rn: Design and assessment of accuracy. *Phys. Chem. Chem. Phys.* 7, 3297. URL: <https://doi.org/10.1039/b508541a>, doi:10.1039/b508541a.
- [65] Weigend, F., Ahlrichs, R., 2005b. Balanced basis sets of split valence, triple zeta valence and quadruple zeta valence quality for H to Rn: Design and assessment of accuracy. *Phys. Chem. Chem. Phys.* 7, 3297–3305. doi:10.1039/b508541a.
- [66] Weininger, D., 1988. SMILES, a chemical language and information system. 1. introduction to methodology and encoding rules. *J. Chem. Inf. Comput. Sci.* 28, 31–36. URL: <https://doi.org/10.1021/ci00057a005>, doi:10.1021/ci00057a005.
- [67] Weinreich, J., Karandashev, K., Arismendi Arrieta, D.J., Hermansson, K., von Lilienfeld, A., 2024. Calculated state-of-the art results for solvation and ionization energies of thousands of organic molecules relevant to battery design. URL: <https://doi.org/10.5281/zenodo.13952172>, doi:10.5281/zenodo.13952172.
- [68] Werner, H.J., Knizia, G., Krause, C., Schwilk, M., Dornbach, M., 2015. Scalable electron correlation methods i.: PNO-LMP2 with linear scaling in the molecular size and near-inverse-linear scaling in the number of processors. *J. Chem. Theory Comput.* 11, 484–507. URL: <https://doi.org/10.1021/ct500725e>, doi:10.1021/ct500725e. PMID: 26580908.
- [69] Werner, H.J., Knowles, P.J., Knizia, G., Manby, F.R., Schütz, M., 2012. Molpro: a general-purpose quantum chemistry program package. *WIREs Comput. Mol. Sci.* 2, 242–253.

- [70] Werner, H.J., Knowles, P.J., Manby, F.R., Black, J.A., Doll, K., Heßelmann, A., Kats, D., Köhn, A., Korona, T., Kreplin, D.A., Ma, Q., Miller III, T.F., Mitrushchenkov, A., Peterson, K.A., Polyak, I., Rauhut, G., Sibae, M., 2020. The Molpro quantum chemistry package. *J. Chem. Phys.* 152, 144107. URL: <https://doi.org/10.1063/5.0005081>, doi:10.1063/5.0005081.
- [71] Werner, H.J., Knowles, P.J., et al., . Molpro, version 2021.1, a package of ab initio programs. See <https://www.molpro.net>.
- [72] Woon, D.E., Dunning, T.H., 1993. Gaussian basis sets for use in correlated molecular calculations. III. the atoms aluminum through argon. *J. Chem. Phys.* 98, 1358–1371. URL: <https://doi.org/10.1063/1.464303>, doi:10.1063/1.464303.
- [73] Zaspel, P., Huang, B., Harbrecht, H., von Lilienfeld, O.A., 2018. Boosting quantum machine learning models with a multilevel combination technique: Pople diagrams revisited. *J. Chem. Theory Comput.* 15, 1546–1559. URL: <https://doi.org/10.1021/acs.jctc.8b00832>, doi:10.1021/acs.jctc.8b00832.
- [74] Zhang, J., Tuguldur, B., van der Spoel, D., 2016. Correction to force field benchmark of organic liquids. 2. Gibbs energy of solvation. *Journal of Chemical Information and Modeling* 56, 819–820. doi:10.1021/acs.jcim.6b00081.